



**Trinity College Dublin**  
Coláiste na Tríonóide, Baile Átha Cliath  
[The University of Dublin](#)

School of Engineering

# CryoSync: Pushing Performance Limits - A Next-Gen Thermal Management Solution for High-Power GPUs

Group 3: Mullally D., Keogh J., Knowles A.,  
Thakur D., Kolekar R.

Supervisor: Prof. A. Robinson

March 11, 2025

MEP55B03 Project 2: Design and Development of Graphics Card  
Cooler

# Contents

<b>1 Executive Summary</b>	<b>5</b>
<b>2 Proposed Technical Approach</b>	<b>6</b>
2.1 Problem Statement and target market . . . . .	6
2.2 Technology/design overview . . . . .	9
2.3 Performance prediction methodology and performance predictions . . . . .	15
2.3.1 Analytical Estimates . . . . .	15
2.3.2 Computational Domain and Governing Equations . . . . .	16
2.3.3 Meshing and Mesh Independence . . . . .	17
2.3.4 Results and Discussion . . . . .	18
<b>3 Design for Manufacture</b>	<b>23</b>
3.1 Materials and Manufacturing . . . . .	23
3.1.1 Materials . . . . .	23
3.1.2 Manufacturing . . . . .	23
3.2 Bill of Materials (BOM) . . . . .	25
3.3 Pricing and Price Point . . . . .	26
<b>4 Technology Appropriateness and Outlook</b>	<b>27</b>
<b>A1 Appendix A</b>	<b>31</b>
A1.1 Thermal Network Analysis . . . . .	31
<b>A2 Appendix B</b>	<b>36</b>
A2.1 Preliminary Design Considerations . . . . .	36
A2.1.1 Jet Design . . . . .	36
A2.2 Fluid Selection . . . . .	38
A2.3 Previous Geometry and Pressure Drop Estimation . . . . .	38
<b>A3 Appendix C</b>	<b>41</b>
A3.1 CFD Results . . . . .	41

A3.2 Future Optimization Work . . . . .	42
---	----

# List of Figures

1.1 CryoSync Cooler . . . . .	5
2.1 CryoSync Top Plate with LED . . . . .	6
2.2 Generic liquid cooler. . . . .	7
2.3 CryoSync Exploded Renders . . . . .	7
2.4 Growth in gaming spend by category . . . . .	8
2.5 Gaming PC market size forecast growth . . . . .	9
2.6 CryoSync Fluid Path . . . . .	10
2.7 Jet Plate and Dimples . . . . .	10
2.8 Top Plate with Decals . . . . .	11
2.9 EcoCirc® Vario Laing D5-38 810 . . . . .	13
2.10 Engineering drawings of CrySync Design . . . . .	14
2.11 Boundary conditions . . . . .	16
2.12 Illustration of computational mesh with mesh refinement levels . . . . .	18
2.13 Surface temperature plot . . . . .	18
2.14 Comparison for analytical and obtained results . . . . .	19
2.15 Pressure plot . . . . .	20
2.16 Pressure drop vs. flow rate analysis for varying pump regimes. . . . .	21
2.17 Power consumption vs. flow rate analysis for varying pump regimes. . . . .	21
3.1 Main Block (center) with steel die cast molds . . . . .	23
3.2 Main Block model with areas marked for post processing in red. Everywhere else will be made during the casting process. . . . .	24
3.3 Jet Plate (center) and steel injection molds . . . . .	25
A1.1 Thermal Network Diagram . . . . .	33
A2.1 Number of Jets vs Heat Transfer Coefficient . . . . .	37
A2.2 Estimated and Obtained Heat Transfer Coefficient for Jets . . . . .	38
A2.3 Simple geometry with flow paths . . . . .	39
A2.4 Final geometry with sections assumed to calculate pressure drop . . . . .	39

A2.5 Estimated Pressure drop for both initial and final geometries (Working Fluid = Water) . . . . .	40
A3.1 Sectioned plot of Velocity . . . . .	42
A3.2 Sectioned orifice plate, highlighting geometric variables . . . . .	43
A3.3 Bottom view of water block for Velocity . . . . .	43

# 1 Executive Summary

The use of graphics cards in computers has become a critical component to be able to handle modern computing programs. Their parallel process capabilities enable them to compute large amounts of data efficiently for high-performance computing, graphical rendering and machine learning. As a result of the increasing power pushed into modern day graphics cards the need for liquid cooling solutions is necessary to satisfy the thermal output, preventing thermal throttling and allowing overclocking. The global market for GPUs is forecast for high growth each year. With the perpetual increase in performance requirements and new graphic card developments there will always be a need for liquid cooling solutions. We at CryoSync have developed a new RTX 3090 cooler that will change the competitive landscape. The sleek and aesthetic design incorporates a high performance jet plate cooler, capable of keeping temperatures low and performance high. It features a modular top plate design to allow users to customize aesthetics to their personal preferences. Combining this with the dynamic pump flow allowing it to adjust the coolant on real time GPU temperatures will inevitably attract a new range of customers. With your financial assistance CryoSync can challenge the industry standards and produce a highly functional GPU cooling system priced at €175. This price was chosen specifically to match current market trends while still maintaining the capacity to generate a healthy profit. It is without any doubt that the CryoSync cooler has high commercial potential with its advanced thermal technology and customization features.

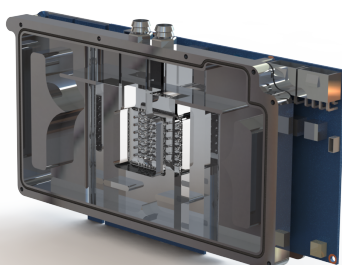


Figure 1.1: CryoSync Cooler

## 2 Proposed Technical Approach

### 2.1 Problem Statement and target market

The CryoSync is a game changing new GPU cooling solution built for dedicated gamers, overclockers, and system builder. Bringing GPU performance to new heights, CryoSync redefines GPU cooling through adaptive cooling and limitless customisation, delivering unmatched performance and personalisation unlike anything on the market.



Figure 2.1: CryoSync Top Plate with LED

#### Problem Statement & Core Challenges

Traditional GPU and PC cooling solutions are widely inefficient, relying on fixed speed pumps that waste energy, generate unnecessary noise, and fail to adapt to the dynamic thermal loads of overclockers and gamers. Beyond this, gamers that buy high-performance components are often left disappointed by the generic, uninspired designs that take away from their unique build aesthetics (see Figure 2.2). We know that the PC gamers we are building for are highly informed consumers who seek maximum value for their dollars. CryoSync directly addresses these shortcomings head-on with intelligent pump control and

easily swapped custom plates. Delivering to gamers a technologically advanced cooling solution that will enhance their dream PC.



Figure 2.2: Generic liquid cooler.

CryoSync's Laing D5 pump intelligently adjusts the coolant flow based on real-time GPU temperatures. This smart regulation system reduces pumping power when you don't need it, allowing us to achieve unmatched efficiency by dynamically reducing the power consumption during idle periods and boosting performance when needed. This functionality, enabled by the Laing D5 pump, allows us to reduce energy consumption by 85% from its maximum capacity. As opposed to competitors products, who operate at these highly inefficient fixed rates, we are a lower energy, quieter, and more sustainable cooling solution. What's more is CryoSync's magnetic top plate customization empowers the 32% of PC gamers who build and 30% who buy custom pre-built machines [1, 2] the opportunity to transform their PC's identity.

### Technical Superiority

At the core of CryoSync's design is a lightweight, die-cast cooling block engineered for superior thermal performance. The split coolant flow path ensures that the GPU die - which contributes to 40.63% of the combined GPU power output - is kept in its ideal operating threshold. The enhanced coolant pathways and pumping power curves, keeps GPU temperatures below a desirable  $36.79^{\circ} C$  under standard 3090 operating conditions.

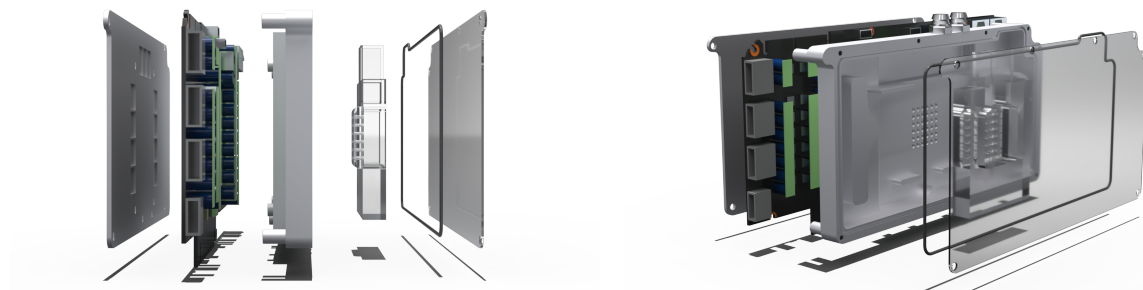


Figure 2.3: CryoSync Exploded Renders

CryoSync leverages cutting-edge jet impingement heat transfer paired with a dimpled heat spreading surface to enhance the turbulent coolant flow over the GPU die, providing high convective heat transfer coefficients of  $38,400\text{W/m}^2\text{K}$ . Jet impingement heat transfer was chosen over alternative technologies for its high heat transfer coefficients at comparatively low pressure drops, providing design flexibility for our dynamic cooling functionality [3]. Thermal performance is further enhanced by an aluminum back plate design which conducts heat from the cooling block and GPU. The additional surface area of the back plate allows the CryoSync to utilize the internal airflow in modern PC enclosures for additional convective dissipation. With the incorporation of leak-proof barbed coolant fittings, quality O-rings, and robust backplate, top plate, and cooling block mounting, the CryoSync design ensures a leak-proof, reliable, and secure cooler assembly.

## Commercial Viability & Market Positioning

CryoSync will disrupt the premium cooling market through its advanced technology and customization at competitive price point of €173.24, catering to the growing number of PC builders prioritizing performance and customization. The PC market is experiencing a trend of growth expected to reach €115 billion by 2030 at a substantial annual growth rate of 12.6% [4]. This is predominantly attributed to the massive rise in the popularity of Esports, as well as VR gaming and AI applications, which is placing increasing demands on hardware components that can sustain the high-performance game play requirements [4]. As the demand for high-performance PC components grows, so too does the cooling solution demand. The growth in gaming spends segmented by category seen in Figure 2.4 clearly highlights PC's substantial contribution to the industry [5].

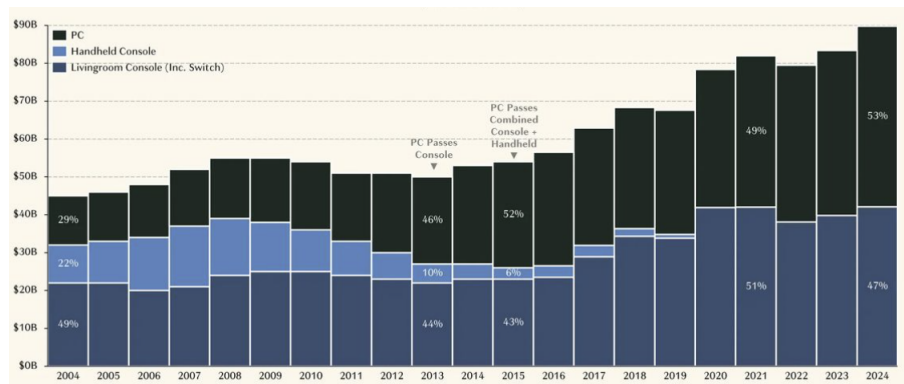


Figure 2.4: Growth in gaming spend by category

CryoSync is designed for the thriving PC gaming market. Since 2021, PC gaming revenue has grown by 20%, surpassing console and laptop gaming revenues. Extensive game libraries, backwards compatibility, and superior performance are the key drivers of this revenue performance [5]. Additionally, approximately 40% of the dedicated PC gamer base

regularly upgrades their hardware every 3.3 years, ensuring steady demand for performance and customization-driven components [2].

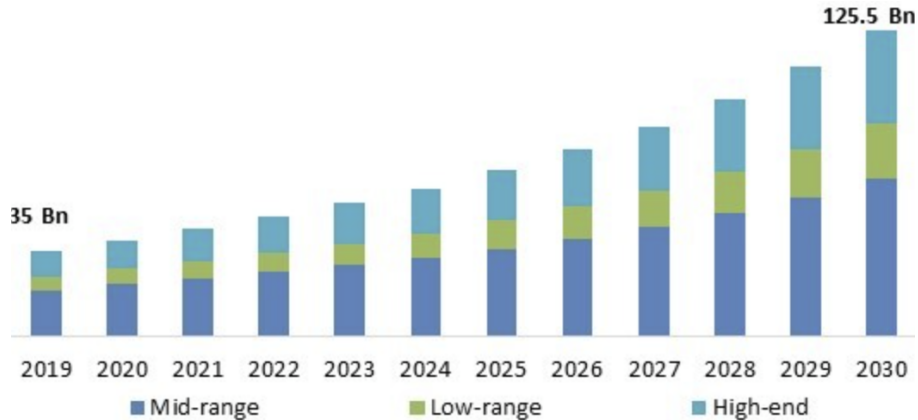


Figure 2.5: Gaming PC market size forecast growth

Recent surveying of PC gamers has shown that just short of one-third of them prefer building custom PCs [2], highlighting the market potential for CryoSync which targets consumer PC building enthusiasts, who seek out customization to add personality to their builds. As mentioned previously, Esports is a substantial driver of the growth in PC gaming. By offering personalized and interchangeable cooler top-plates, our customers can support their favorite Esports teams while achieving the high performance required from their hardware, enabled by our superior thermal performance.

## 2.2 Technology/design overview

The CryoSync water block is a majority aluminum construction. It measures 190 mm x 20.5 mm x 98 mm. The fluid path first reaches the GPU die. This was chosen as the heat flux from the GPU die is nearly 5 times the amount of the next highest heat flux (GPU: 20.06 w/cm<sup>2</sup>, VRM: 4.53 w/cm<sup>2</sup>). In order to hit the GPU die first, the water block makes use of a split flow design. After the GPU die, the coolant splits in two major directions to cool the rest of the components before joining back at the coolant outlet. The flow path can be seen in Figure A2.4. Both inlet and outlet make use of barbed fittings to enable easy installation with a leak-free connection.

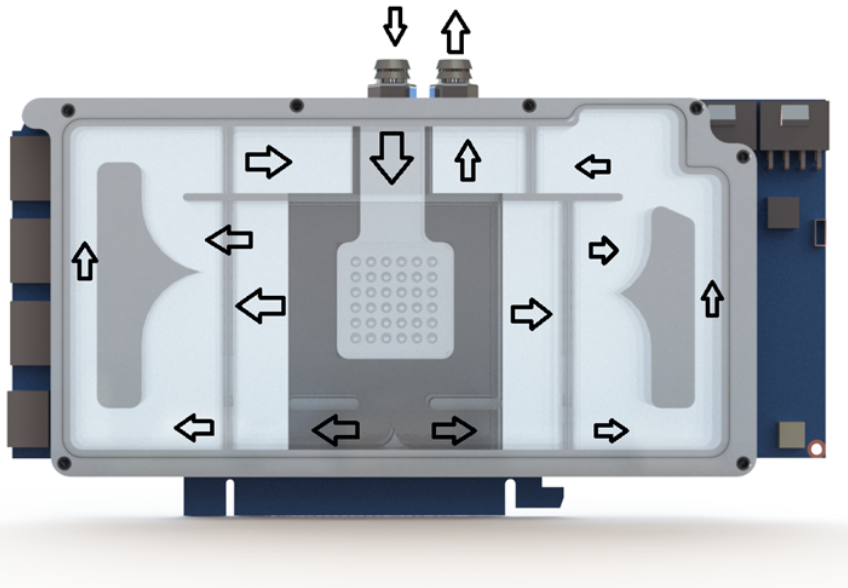


Figure 2.6: CryoSync Fluid Path

A backplate is used on the rear of the GPU to act as a stiffener and a heat spreader for the components on the back. Due to the large surface area of the backplate and limited heat flux produced by these components, it is more than sufficient to cool this with convection in the PC case. Two advanced cooling systems work in conjunction to cool the GPU die: a jet impinging array and a dimpled heat spreader. These work together to direct high-velocity jets of coolant to the dimpled heat spreader. The direct impact of the jets enhances the heat transfer when compared to traditional water blocks. It creates localized cooling while promoting turbulence generation at the impact points. This disrupts the boundary layer and further improves cooling performance. The dimples were added in order to increase the surface area and have the potential to promote vortex formation.

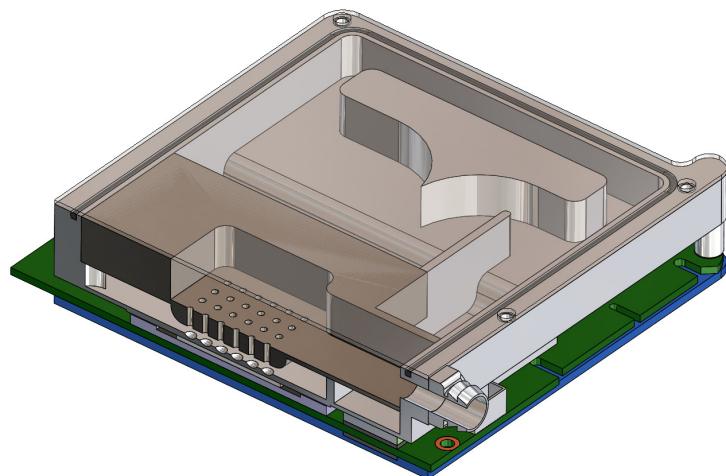


Figure 2.7: Jet Plate and Dimples

The CyroSync makes use of a number of thermal interface materials (TIMs) to increase thermal transfer from the heat-generating components to the aluminium block. As the GPU die creates the most heat, a thermal paste is used to ensure good surface contact while keeping operating temperatures low. The VRMs, VRAMs, and capacitors use a thermal pad. This allows for easy application while also bridging the 0.5 mm gap between the components and the block.

Two separate USPs make the CryoSync stick out from the competition. Many gamers have started to mount their GPUs vertically to show off their GPUs in their tempered glass PC cases. One way that CryoSync stands out is the optional customizable top plate. This plate is mounted to the GPU using magnets. The top plate can be customized and easily changed without the need for disassembly of the water block. CryoSync offers a number of options: decal top plates, dye sublimation, and laser-cut top plates.

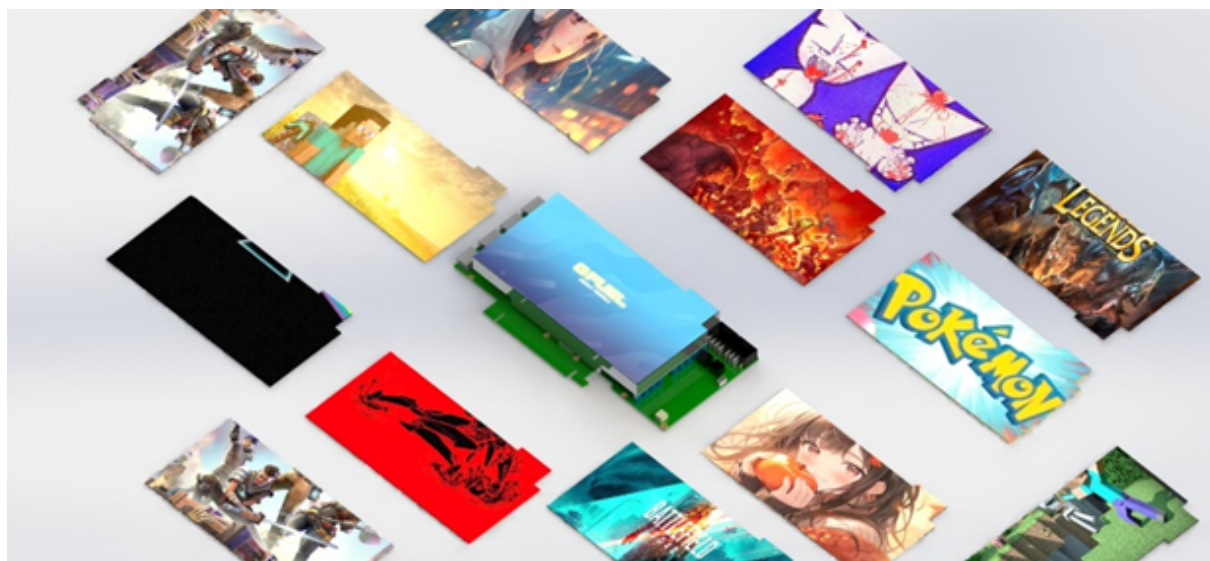


Figure 2.8: Top Plate with Decals

These can be customized to the customer's liking, showing off their favorite game or TV show, their gamer-tag, or even an Esports team logo. The options are endless, only limited by the imagination of the customer.

## Dynamic Cooling

The second performance selling point of the CryoSync is its integrated dynamic pump speed control. This functionality offers significant improvements to cooling power efficiency, hardware longevity, and user experience. Traditional GPU cooling solutions on the other hand implement "fixed-speed" pumps that maintain a constant flow rate regardless of the electronics thermal loads, drawing unnecessary power and increasing the acoustic annoyance.

The fundamental equation for the heat transfer capacity of a fluid is simply defined as,

$$Q = \dot{m}c_p\Delta T \quad (2.1)$$

or,

$$Q = \rho \dot{V} c_p \Delta T \quad (2.2)$$

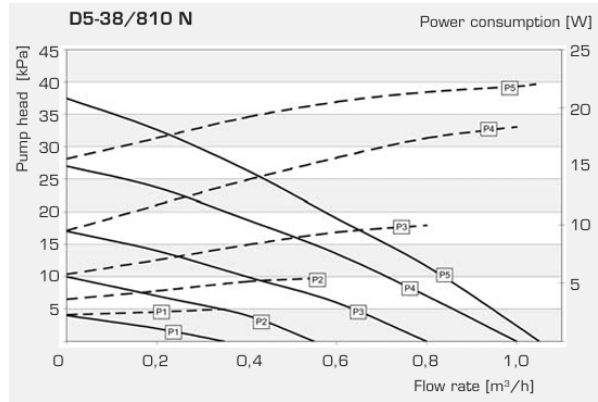
From this equation we see that by modifying the volumetric, or mass flow rate of the coolant we can directly adjust the cooling power applied to the GPU. At low GPU power demands we can reduce the flow rate and for high thermal stress applications with increased power and transients we can effectively increase the flow rate to reduce the temperature spikes within the chip. There were two possible approaches to manipulating the supplied coolant flow rate; the first was to implement a throttling valve at the inlet to manually interrupt the fluid and reduce the flow rate. This was not the chosen approach. For a fixed pumping power, a reduction in mass flow rate- through throttling- must be accompanied by a corresponding pressure drop as highlighted in Equation 2.3. Therefore, dynamically adjusting the cooling power by restricting the flow would inevitably result in substantial energy losses through increased resistance, counteracting our energy efficiency objectives.

$$P = \frac{\dot{m}}{\rho} \Delta P \quad (2.3)$$

To address this, CryoSync implements real-time variable pumping power, providing dynamic flow rate adjustment to respond to the variable GPU thermal demands. The CryoSync leverages the Laing EcoCirc® Vario D5-38 810 pump to achieve this, seen in Figure 2.9 [6]. Laing D5 pumps are a market leading, compact and lightweight fluid pump solution used widely in industrial, computer and medical cooling applications. The integrated speed controller allows for precise adjustment of hydraulic performance or power consumption with 5 primary primary operating regimes shown in Figure 2.9(b). The EcoCirc® also implements sine wave commutation, allowing silent operation at high output levels [6].



((a)) EcoCirc® Vario Pump Exploded View



((b)) Laing D5 Pump Curves

Figure 2.9: EcoCirc® Vario Laing D5-38 810

The responsiveness of the CryoSync to the real-time GPU thermal loads allows us to target and mitigate rapid temperature fluctuations of the GPU die under varying computational loads associated with gaming, rendering or other high demand applications. Dynamic smoothing of temperature peaks - which are known to cause thermal stress and potential hardware degradation - ensures enhanced GPU longevity and sustained peak performance. In industry and academia, computational scheduling and parallel computing algorithms are in development to prevent these transient overpowering and overheating of GPU and CPU components in high power applications. Lee et al. notes that a  $6 - 12.2^{\circ}\text{C}$  reduction in maximum chip temperatures can result in a 1.5 X improvement in chip lifetime reliability [7]. Through dynamic cooling adjustments, CryoSync provides additional cooling headroom to reduce the transient overheating effects and subsequently reduce power consumption when steady state thermal loads are reached.

From CFD analysis of the thermal behavior of the CryoSync, described in Section 2.3.4, we have outlined initial operating regimes for the CryoSync. In operation, CryoSync will extract temperature data from the onboard thermal diodes for real-time temperature regulation and through software updates we will have the ability to further tune this algorithm over time. The Laing D5 pump operates between five speed control settings; P1 (1800 rpm), P2 (2550 rpm), P3 (3300 rpm), P4, (4050 rpm), and P5 (4800 rpm). As will be discussed in the later section 2.3.4, varying between several operating set points allows us to significantly reduce energy and operate at lower motor speeds increasing the longevity of our GPU and pump system.

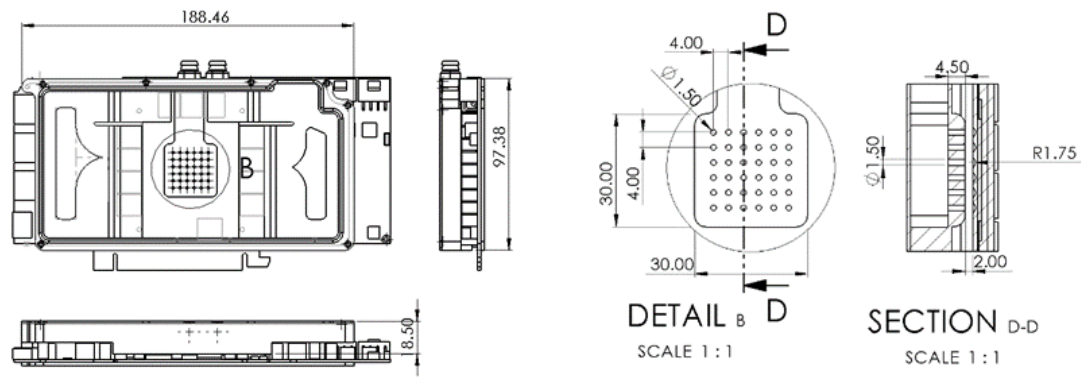


Figure 2.10: Engineering drawings of CrySync Design

## 2.3 Performance prediction methodology and performance predictions

CryoSync was designed to cool Nvidia RTX 3090, producing around 320 W with the maximum pressure drop of around 11 kPa. (refer A2 for details regarding detailed calculations). The following assumptions were taken while designing GPU cooling block.

Components	Values	Unit
GPU Chip	130	W
VRAM	70	W
Capacitor	40	W
VRM	60	W
Other Components	20	W

Table 2.1: Power distribution on the RTX 3090

Parameters (Water)	Values	Units
Inlet Temperature	27	°C
Dynamic Viscosity	0.00086	Pa·s
Density	996.38	kg/m <sup>3</sup>
Thermal Conductivity	0.6096	W/m
Heat Carrying Capacity	4181	J/kgK
Kinematic Viscosity	8.6151E-07	m <sup>2</sup> /s

Table 2.2: Analytical Design Assumptions

### 2.3.1 Analytical Estimates

Jets were designed by referring to the work of Robinson J. [3] and Elliott *et. al.* [8]. By studying various jet arrangements and dimensions, it was finalized to use a 1.5 mm jet diameter with jet-to-jet spacing (S/D where S is the spacing between jets and d is the diameter of jets) of 2 mm; thus, 30 jets were fitted over the GPU chip of 648 mm<sup>2</sup> area. The distance between the jet plate and the surface of the cooling face was kept at 2 mm.

Pressure drop along the overall GPU die was estimated by,

$$\Delta P = f \cdot \left( \frac{1}{2} \rho V^2 \right) \cdot \frac{L}{D_H} + K \cdot \left( \frac{1}{2} \rho V^2 \right) \quad (2.4)$$

where,  $\rho$  is the density of the fluid ( $kg/m^3$ ),  $V$  is the velocity of the fluid ( $m/s$ ),  $L$  and  $D_H$  are the lengths of the channel and the hydraulic diameter of the channel ( $m$ ),  $K$  is the minor loss coefficient,  $f$  is the friction factor, which is estimated by using the Reynolds number ( $Re$ ),

$$f = 0.51 + \frac{229.9}{Re} \quad (2.5)$$

### 2.3.2 Computational Domain and Governing Equations

A representation of the computational domain for the simulation case is depicted in Figure 2.11, showing both fluid and solid subdomains. Material for the water block was aluminum 6061, except for the top cover plate, which was acrylic. The GPU chip was silicon, ceramic for capacitors, and equivalent materials were applied for the other remaining components of the GPU board.

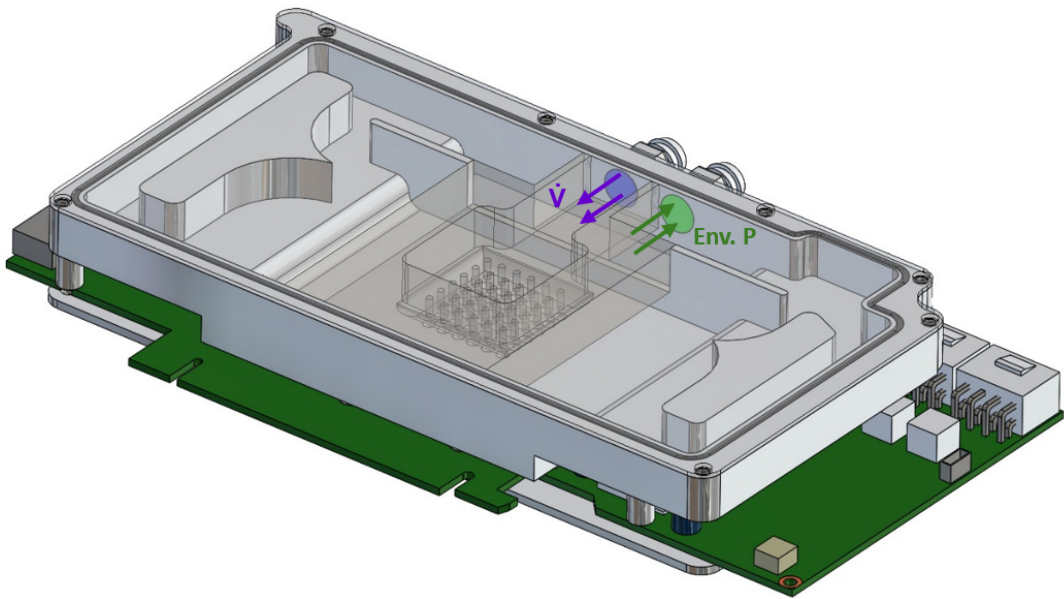


Figure 2.11: Boundary conditions

The boundary conditions for the CFD model are as follows; a uniform heat transfer rate, representative of the heat produced from the GPU chip, VRM, VRAM, capacitors, and other components as shown in Figure 2.1 was applied to the particular heat source components. An environmental pressure boundary condition was applied at the outlet nozzle, whilst a mass flow rate was applied at the inlet. The flow rates were varied between fixed flows of 0.00065 - 0.14 Kg/s.

The computational domain is solved for fluid flow and heat transfer with the k- $\epsilon$  turbulence model in SolidWorks. The commercial software package SolidWorks is used to solve the steady-state conservation equations for mass, momentum, and energy within the fluid domain. These are as follows [9]:

Conservation of mass:

$$\frac{\partial \rho}{\partial t} + \frac{\partial(\rho u_i)}{\partial x_i} = 0 \quad (2.6)$$

Conservation of Momentum:

$$\frac{\partial(\rho u_i)}{\partial t} + \frac{\partial}{\partial x_j}(\rho u_i u_j) + \frac{\partial P}{\partial x_i} = \frac{\partial}{\partial x_j}(\tau_{ij} + \tau_{ij}^R) + S_i \quad (2.7)$$

Conservation of Energy:

$$\frac{\partial \rho H}{\partial t} + \frac{\partial \rho u_i H}{\partial x_i} = \frac{\partial}{\partial x_i} (u_j (\tau_{ij} + \tau_{ij}^R) + q_i) + \frac{\partial p}{\partial t} - \tau_{ij}^R \frac{\partial u_i}{\partial x_j} + \rho \varepsilon + S_i u_i + Q_H \quad (2.8)$$

Where,

$\rho$  = Fluid density

$u$  = Velocity vector

$p$  = Pressure

$\mu$  = Dynamic viscosity

$H$  = Enthalpy

### 2.3.3 Meshing and Mesh Independence

A mesh independence study was carried out using SolidWorks to ensure accurate and reliable simulation results. The mesh density is increased incrementally until the key variables such as GPU temperature and pressure converge sufficiently. As shown in the Figure 2.12, the mesh is well refined to optimize computational resources and precision. To resolve the fine scale thermal and flow gradients, the highest mesh density was used immediately surrounding the jets. In order to ensure maximum accuracy around the impinging jets, a localized mesh region was created to better capture the turbulence and high gradients in the region where the jets impinged on the target surface. The mesh independence study was carried out using the baseline design for the flow rate of 0.069 Kg/s. Table III indicates that a mesh of approximately 2.8 million cells was sufficiently dense, since the difference between tracked variables (overall pressure drop and GPU temperature shown here) was less than 1% with the next highest mesh count.

Parameter	Mesh 1	Mesh 2	Mesh 3	Mesh 4
No of Elements ( $\times 10^6$ )	1.33	2.14	2.80	3.94
Difference in GPU Temperature (%)	-	0.317	0.007	0.006
Pressure Difference (%)	-	0.984	0.020	0.010

Table 2.3: Mesh Independence Study

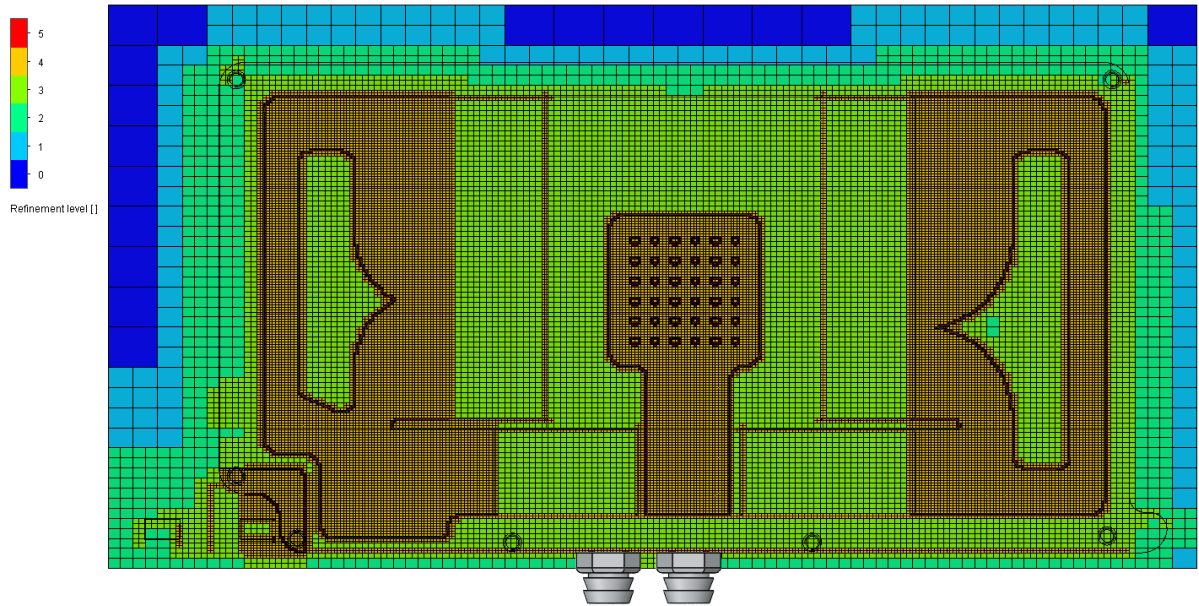


Figure 2.12: Illustration of computational mesh with mesh refinement levels

### 2.3.4 Results and Discussion

After conducting a series of computational fluid dynamics (CFD) simulations across a range of flow rates, we identified an optimal flow rate of 0.12 kg/s for the cooling system of the Nvidia RTX 3090. This flow rate effectively maintains the average GPU surface temperature at a remarkably low 36.3 °C, with a peak temperature of just 37.23 °C as shown in Figure 2.13.

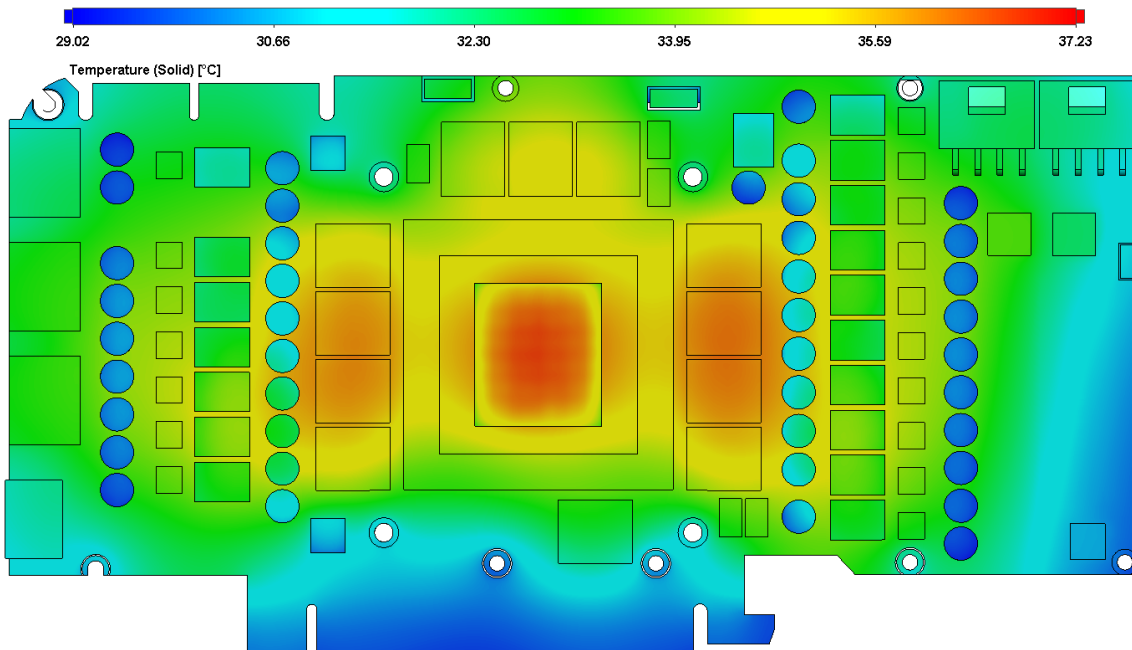


Figure 2.13: Surface temperature plot

These temperatures significantly undercut the critical thresholds for GPU performance, ensuring both enhanced functionality and reliability during extensive gaming sessions.

Additionally, the system exhibits a pressure drop of 9030 Pa, indicative of the resistance within the coolant flow paths. Despite this, the pressure remains manageable within the capabilities of the specified Laing D5 pump, ensuring efficient operation.

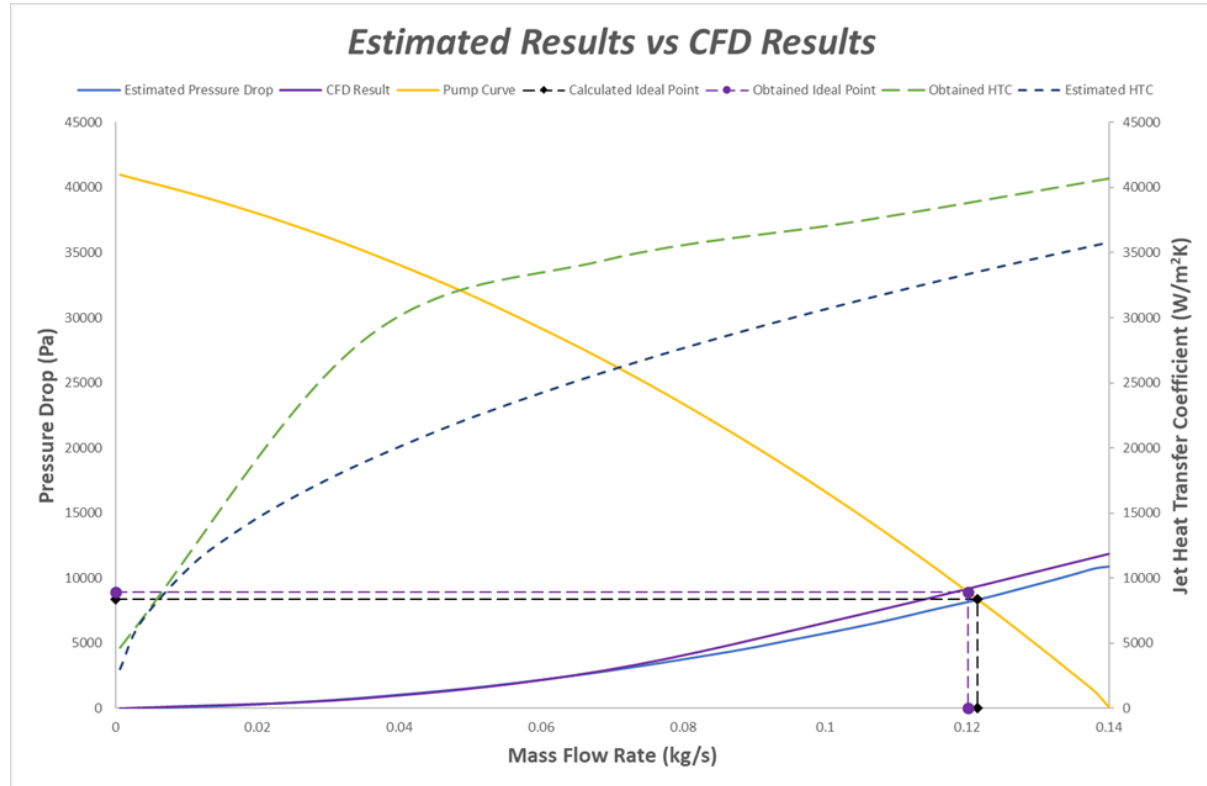


Figure 2.14: Comparison for analytical and obtained results

Fig.2.14 shows the comparison between analytical and CFD results, with both indicating the ideal point for flow to be close to 0.12 kg/s. It also indicates that the assumed values for K (minor loss coefficient) are good enough and that flow and pressure drop are predictable using the approach; details are present in A2. Fig.2.14 also shows a comparison for the heat transfer coefficient for jets. For the ideal point, estimated coefficient was around 33831.75 W/m<sup>2</sup>K, whereas the CFD result shows it to be 38413.114 W/m<sup>2</sup>K. This gap is supposed to be due to the presence of dimples which were added to increase surface area and promote vortex formation. As it increases surface area, it improves the heat transfer coefficient as well. The figure of merit was also calculated by using,

$$FOM = \frac{1}{(T_{GPU} - T_{Coolant})^3(T_{max} - T_{Coolant})^{1/3}(\dot{V}\Delta P)} = 5.26 \times 10^{-7} \quad (2.9)$$

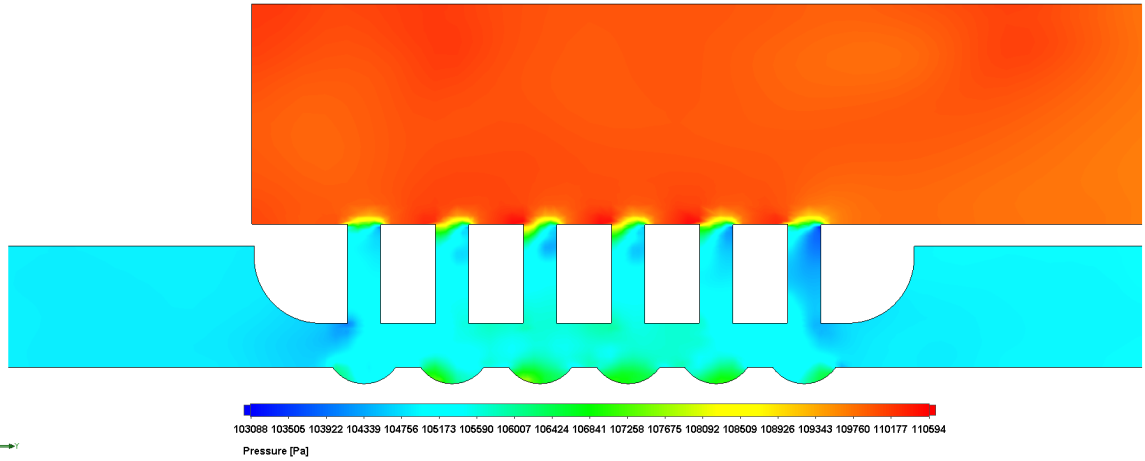


Figure 2.15: Pressure plot

Figure 2.15 illustrates the pressure distribution across the water block cooling system, focusing particularly on the area of the jet orifices. The plot reveals a relatively uniform pressure distribution in the chamber area. This uniformity is crucial as it ensures that each cooling jet receives an equivalent driving force, leading to a consistent and uniform distribution of coolant flow across all jets.

### Variable Pump Power Implementation

As described in Section 2.2, the CryoSync implements a variable flow rate pump to deliver power savings, efficiency and GPU longevity by adapting the cooling power to the GPU requirements. By applying the five pump and pressure loss curves seen in Figure 2.9 to the achieved results, we can investigate the possible energy savings and ideal operating regimes for the CryoSync. Applying the hydraulic and thermal analysis carried out in the previous section, we can inform the ideal steady-state operating setting of the pump. The updated flow rate vs. pressure drop and corresponding electrical pumping power analysis can be seen in Figures 2.16 & 2.17.

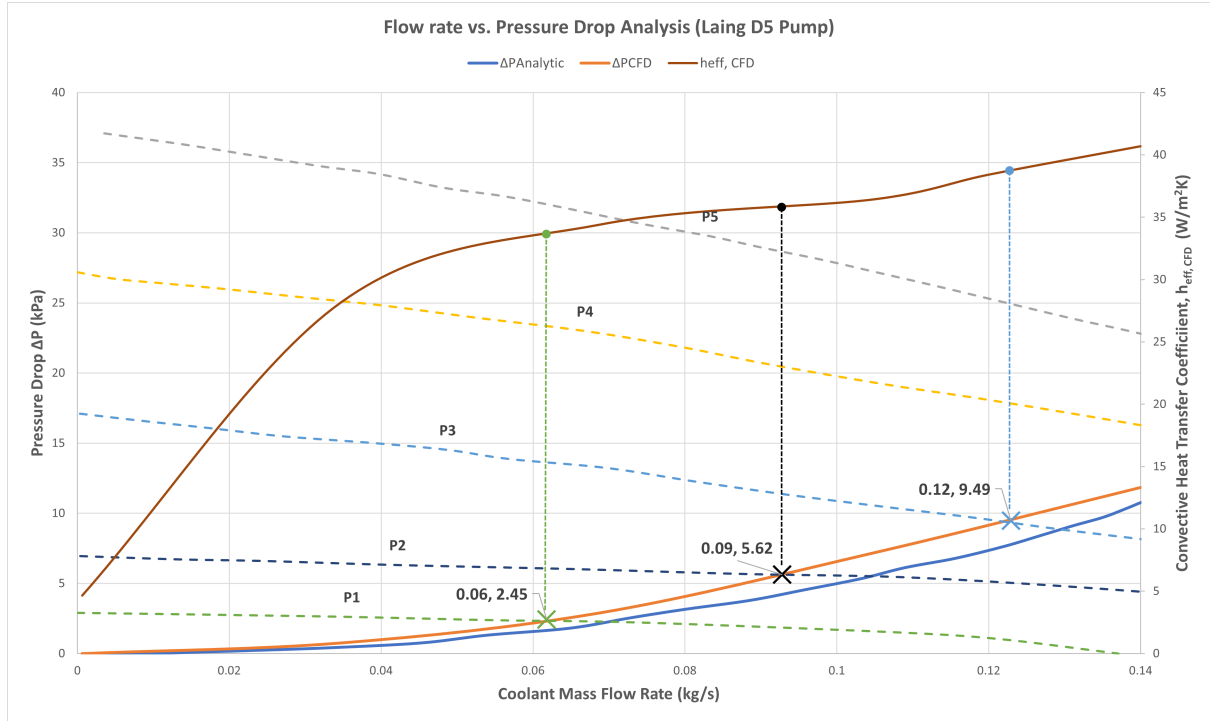


Figure 2.16: Pressure drop vs. flow rate analysis for varying pump regimes.

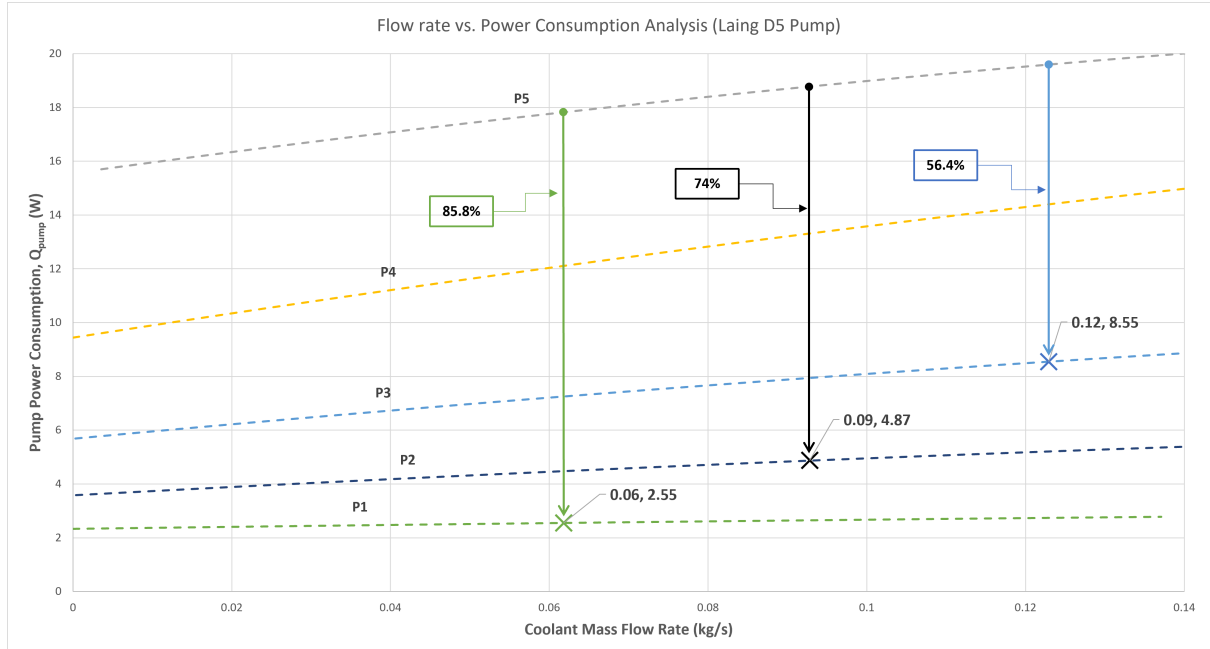


Figure 2.17: Power consumption vs. flow rate analysis for varying pump regimes.

Denoted by crosses in Figure 2.16, we see that now for the target GPU die power (130 W), it is possible to operate within the three lowest operating regimes: P1, P2, & P3. The P3 operating regime will maintain the best performance with a maximum GPU die temperature of  $35.85^{\circ}\text{C}$ ; however, operation in the P1 regime will result in a minor increase in GPU die temperature of  $2.52^{\circ}\text{C}$ , for further significant reduction in power consumption by 46.65%, as

seen in Figure 2.17. The ability to operate at lower flow rates with reduced pressure drops can be attributed to the high heat transfer coefficient of the impinging jet array with low pressure drop penalties.

The advantages of dynamically adjusting the pumping power are clear in Figure 2.17. By moving away from the industry standard of constant operation at maximum power to accommodate all possible GPU loading, we are able to save between 56.4 – 85.8% in power consumption by decreasing the flow rate whilst still maintaining satisfactory GPU temperatures. This is a reduction of between 11.25 – 15.37 W. If the GPU is operated for one hour a day over the course of one year, that would result in substantial energy savings between 14.78 & 20.20 MJ. Although our current design allows us to provide sufficient cooling power at the lower operating regimes of the Laing pump, the possibility of increasing the pumping power to the P4 & P5 regimes means that we can enable overclocking and thermal peak reduction by supplying surplus power to increasing the flow rate. In conclusion, the combination of the jet impingement array and flexible pump operation allows the CryoSync to operate efficiently while catering to the most extreme thermal cycling. Although this will incur additional costs, the GPU longevity and power consumption reductions make this a highly attractive approach.

# 3 Design for Manufacture

## 3.1 Materials and Manufacturing

### 3.1.1 Materials

The cooling block that forms the main component of the assemble, is made with aluminum 1060. This metal is widely used in CPU heatsinks due to its high thermal conductivity, and relatively low cost to other thermally conductive metals (copper, etc). As seen in the manufacturing section, this metal is suitable for die casting (Figure 3.1). This gives an advantage for high volume production where overtime, the cost per unit will reduce. Alternatively, if there is a limited production run of the product, CNC machining can be done.

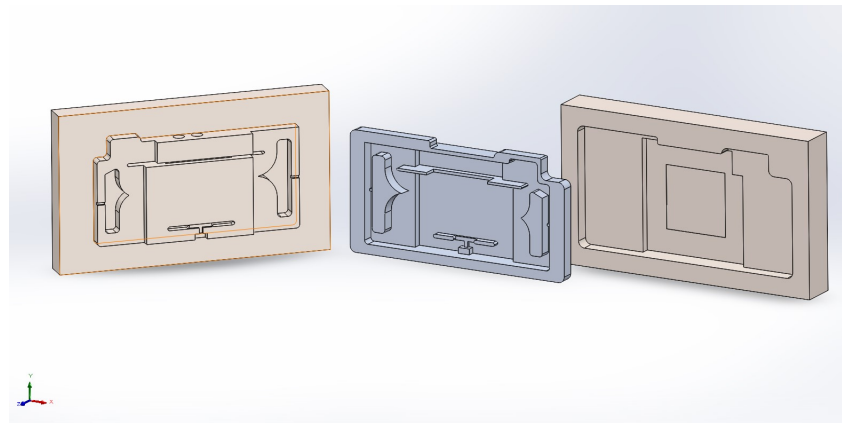


Figure 3.1: Main Block (center) with steel die cast molds

The top plate, back plate and jet plate are all made with acrylic.

### 3.1.2 Manufacturing

When deciding on the manufacturing process to produce the main aluminum block, some considerations were given to the use of sheet metal pressing techniques. This is a low-cost process that can give the product a competitive edge in terms of cost reduction. However, the profile of the main block varies in thickness, where at minimum it is 1mm, and at

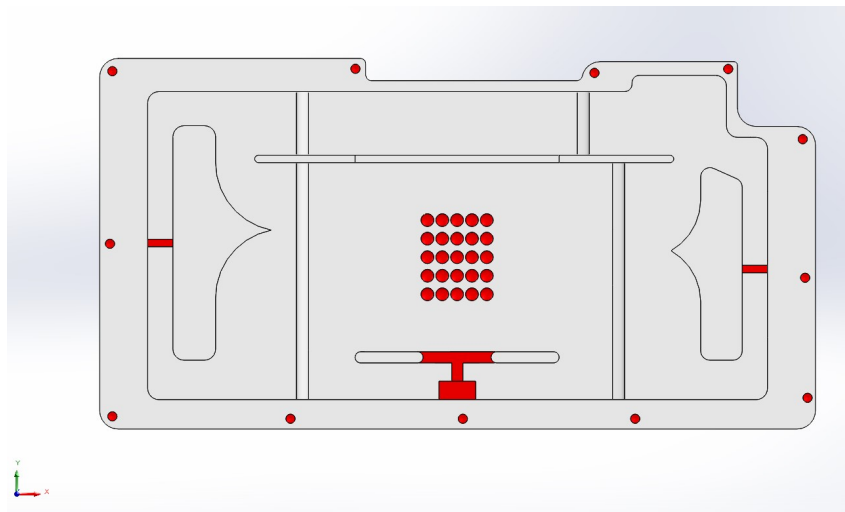


Figure 3.2: Main Block model with areas marked for post processing in red. Everywhere else will be made during the casting process.

maximum 11mm. This makes the design unfeasible for stamping/pressing techniques because aluminum sheets cannot be used. Therefore, the workpiece cannot be a sheet. 3 axis milling was another process that was considered, which is suitable for low-volume production. For higher volume production, this method will be commercially unsustainable and will have a high material wastage.

It was decided to use die casting for the main block, along with machining in the post-processing. Die casting aluminum, with steel dies, can produce accurate parts with a smooth surface finish. Figure 3.2 shows a simplified model of the main block, with holes and vanes removed/filled (shown in red). For the isolated extrusions, they were connected to the walls with runners, otherwise they will not be filled. The runners will also have to be machined through milling. These post-processing steps can be achieved with a 3 axis CNC machine. The smallest space that needs to be machine is 6.5mm long, thus any milling tool needs to be <6.5mm in diameter. The drill holes must be M2.5 and tapered. Finally, the holes for the ports (large red circles in Figure 3.2), will need to be drilled with a M9 drill bit.

The back plate, another aluminum part, has a uniform thickness of 2mm. This part can be made with a laser cutting machine, milling for the grooves and drilling with a M2.5 drill bit. Alternatively, all the steps can be done with the laser cutter, however there is a risk of warping which may affect the material properties. The 9mm standoffs can be purchased in bulk.

The Jet Plate is made of acrylic and has a simpler geometry than the main block. This part can be manufactured with die injection molding. Ideally, the part would not need post processing, however, the cone shape of the holes will be difficult to cut in a 3 axis machine. The close proximity of the holes and cone bases (less than 1mm between the bases) restricts type of tools that can be used to machine this space. To work around it, the mold will have

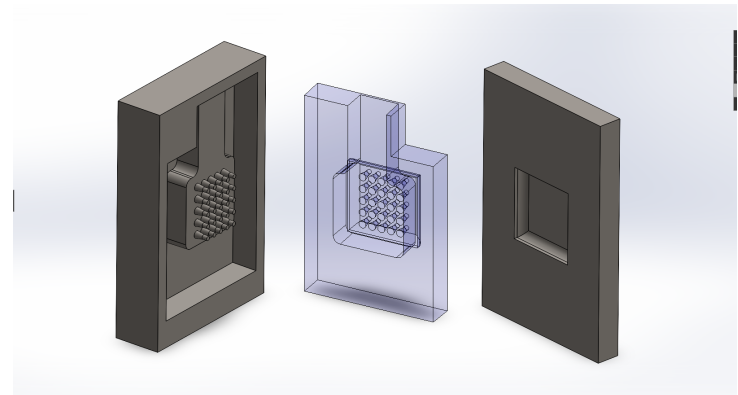


Figure 3.3: Jet Plate (center) and steel injection molds

straight holes, then after casting, the cone holes can be machined with a cone drill bit.

The top will be made with acrylic sheets (1mm thick), that can be cut with a laser cutting machine. The M2.5 holes can be cut with the laser as well. This will help keep all steps of the process on the one machine, without any change over to another system. Given the length of the plate is 19cm, multiple plates can be cut from the same sheet.

## 3.2 Bill of Materials (BOM)

This section includes the total costs of all of the materials required for the products, the quantities of these products needed, and the total cost of the materials needed for manufacturing the product. There are also estimations for the cost of machining and casting with each part. There is also the cost of creating the molds. The die casting is assumed to be contracted to a foundry that has the equipment, whom the molds will be sent to, thus the capital costs of the machinery is omitted.

Components	Material	Material Cost	Mass (kg)	Qty	Total Cost (€)
Main Block	Aluminium 1060	€2.8/kg	0.247	1	€0.69
Back Plate	Aluminium 1060	€2.8/kg	0.09636	1	€0.27
M2.5x9 Standoffs	Aluminium 1060	€0.5/100	-	4	€0.02
Jet Plate	Acrylic	€1.35/kg	0.04354	1	€0.0588
Top Plate	Acrylic	€1.35/kg	0.022	1	€0.0297
M2.5x6 Screws	Steel	€0.1205/screw	-	16	€1.93
M7 Hose Connector	Steel	€2.65/unit	-	2	€5.3
Labour	-	€35/unit	-	-	€35
<b>Total</b>					<b>€43.40</b>

Table 3.1: Bill of Materials for the product.

While the total cost of the materials is low, there is also the associated costs of labour and machining. This will increase the cost of production considerably. If the cost of machining were to be €70 per hour (includes energy and labour cost), this includes the costs for the 3 axis CNC, die casting and laser cutting each. For two die casts, two laser cutters, and one 3

axis CNC, the total machine costs are €350. If say 10 units are produced per hour, then the machine cost per unit is €35. Add the material cost described in the BOM, the total cost per unit is €43.395. These costs are optimistic and may be higher.

### 3.3 Pricing and Price Point

The cost of the cooler is low, which does not include the capital costs of the die casting and other equipment. Looking to the market, a benchmark price can be found. On the upper end of the price range is the Corsair Hydro X Series at €211 and the Phanteks Glacier at €226.52. In the lower price range, many generic brands price their water blocks between €20 - €40, however the quality of these devices is not guaranteed. Suppose the costs per unit are underestimated, we can take the median value between these ranges, €133.26. The expected volume of cooling blocks to be produced is 1 million units. The expected revenue is thus 133.3 million euros. In order to breakeven and account for uncertainty in the product costs, a markup of 30% will help cover the capital costs and turn over a profit. Thus the final price is €173.24 and the revenue is 173 million euro.

## 4 Technology Appropriateness and Outlook

The CryoSync liquid cooler is a practical, forward-thinking solution to what is an apparent downside to most market GPU liquid coolers: a lack of customization and poor operating efficiency. Its core features of adaptive cooling control and customization aesthetics are incorporated more frequently in CPU cooling, which highlights the opportunity to cross-pollinate these features to the GPU market as it is poised for rapid growth. The implementation of the Laing D5 variable-speed pump, with proven reliability and quiet operation, enhances the product's appeal to gamers seeking both performance and efficiency.

CryoSync aligns well with the current market demands and trends, particularly the rising popularity of high-performance custom PC building with high-powered graphics cards requiring tailored cooling solutions. The primary innovation of intelligent cooling control allows for the effective cooling of the Nvidia 3090—one of the most computationally intense cards on the market—with significantly reduced power consumption. This technological achievement is enabled by the incorporation of an impinging jet array to provide substantial heat transfer capacity to the system. CryoSync's implementation of a jet-impingement array presents the opportunity for further design opportunities in more compact or optimised form factors. By achieving energy savings without compromising on thermal performance, CryoSync is a highly affordable and innovative offering for €173.24.

### Scalability & Outlook

CryoSync's scalability is highly promising; leveraging cost-effective manufacturing techniques like die-casting, CryoSync will be able to meet the demands of the forecast sales. Using affordable and widely-available materials, CryoSync is entering the market at a price point within the lower bracket of premium liquid cooling solutions. This represents an attractive value proposition for consumers, providing strong initial market penetration to further expand into broader applications while developing manufacturing capabilities. Strategic partnerships with popular brands and Esports teams to sell custom top plates enhance our exposure and

position CryoSync as an interesting alternative to mundane market alternatives.

Distribution through the major PC component retailers such as Amazon, Newegg, and Micro Centre in North America, alongside direct-to-consumer sales channels, ensures maximum reach. Maintaining a supplementary direct-to-consumer model will enable increased margins as our share of the market and brand notoriety increase. A key marketing and distribution strategy that CryoSync will explore is the exposure to the massive audiences of key PC and PC gaming influencers like Linus Tech Tips and Gamers Nexus. YouTube influencers like Jayztwocents, who receive 9 million monthly views, frequently upload liquid cooling reviews, providing unprecedented exposure. The lack of distinct branding and targeted marketing in the liquid cooling sector represents a significant opportunity to differentiate from our competitors. This is expected to be a key avenue to growing CryoSync's brand presence.

In conclusion, CryoSync exhibits strong technological appropriateness and commercial viability to capture the gaming PC market by offering excellent thermal performance and enabling greater personalisation.

# Bibliography

- [1] A. Patrizio, "Gamers and PC enthusiasts are spending up to \$25,000 to deck out their setups — and components makers are jumping on the trend." [Online]. Available: <https://www.businessinsider.com/inside-world-pc-computer-modding-gamers-deck-out-setups-2021-9>
- [2] "Demand for PC Hardware Has Skyrocketed: Who Are the Gamers Looking to Upgrade? What Motivates Consumers to Spend?" Dec. 2021. [Online]. Available: <https://newzoo.com/resources/blog/demand-for-pc-hardware-has-skyrocketed-who-are-the-gamers-looking-to-upgrade-what-motivates-consumers-to-spend>
- [3] A. Robinson, "A thermal–hydraulic comparison of liquid microchannel and impinging liquid jet array heat sinks for high-power electronics cooling," vol. 32, no. 2, pp. 347–357. [Online]. Available: <http://ieeexplore.ieee.org/document/4801567/>
- [4] "Gaming PC Market Size, Share & Top Key Players by 2023-2030." [Online]. Available: <https://www.kbvresearch.com/gaming-pc-market/>
- [5] L. C. published, "New report says PC games are outselling console games, calling PC gaming a 'bright spot' in a troubled industry," *PC Gamer*, Jan. 2025. [Online]. Available: <https://www.pcgamer.com/gaming-industry/new-report-says-pc-games-are-outselling-console-games-calling-pc-gaming-a-bright-spot-in-a-troubled-industry/>
- [6] Laing GmbH, "Ecocirc vario dc pumps: Technical data and applications," <https://laing-pumps.com>, Remseck, Germany, accessed: 2025-03-09. [Online]. Available: <https://docs.rs-online.com/0900766b80f08f97.pdf>
- [7] Y. Lee, K. G. Shin, and H. S. Chwa, "Thermal-Aware Scheduling for Integrated CPUs–GPU Platforms," *ACM Transactions on Embedded Computing Systems*, vol. 18, no. 5s, pp. 1–25, Oct. 2019. [Online]. Available: <https://dl.acm.org/doi/10.1145/3358235>
- [8] J. Elliott and A. J. Robinson, "Optimised liquid impinging jet arrays for cooling CPU packages," pp. 1–1. [Online]. Available: <https://ieeexplore.ieee.org/document/10731867/>

- [9] D. A. S. Dr. A. Sobachkin, Dr. G. Dumnov, “Numerical basis of cad-embedded cfd.” [Online]. Available: [https://www.solidworks.com/sw/docs/Flow\\_Basis\\_of\\_CAD\\_Emb\\_edded\\_CFD\\_Whitepaper.pdf](https://www.solidworks.com/sw/docs/Flow_Basis_of_CAD_Emb_edded_CFD_Whitepaper.pdf)

# A1 Appendix A

## A1.1 Thermal Network Analysis

Variable	Name	Unit
$T$	Temperature at a given node	°C
$Q$	Heat transfer rate	W
$R$	Thermal resistance	K/W
$R_{TIM, GPU}$	GPU TIM Thermal Resistance	K/W
$k$	Thermal conductivity	W/m·K
$h$	Convective heat transfer coefficient	W/m <sup>2</sup> ·K
$h_{conv, imp}$	Impinging jets effective heat transfer coefficient	W/m <sup>2</sup> ·K
$A$	Surface area for heat exchange	m <sup>2</sup>
$L$	Characteristic length for conduction	m
TIM	Thermal Interface Material	-
VRAM	Video random access memory	-
VRM	Voltage regulator module	-
CAP	Capacitors	-
WB	Water Block	-
C	Coolant	-

Table A1.1: Nomenclature for Thermal Network

A thermal network analysis was carried out, as shown in Figure A1.1, to analytically analyse the thermal pathways between the GPU components and the coolant flow. To simplify this analysis, several approximations were made. Firstly, convection and radiation to the surroundings are ignored; this includes the conduction and convective dissipation provided by the back plate. This will, in reality, reduce the overall resistance of the system; however, for a worst-case analysis, by ignoring these contributions, we can isolate the thermal resistance between the components and the coolant. Secondly, for simplification in the diagram, it is assumed that the water block is isothermal when steady state is reached and is thus treated

as a singular temperature node. In reality this is not a perfect assumption; the thermal resistivity associated with the jet impingement convection is lower than the conduction through the aluminium water block, and this assumption of isothermal temperatures is not entirely valid.

### **Thermal Conductivity of Aluminium**

$$k_{AL} = 167 \text{ W/mK}$$

### **Effective conductance of Impinging Jets**

$$h_{Imp,Jet} = 33831.75 \text{ W/m}^2\text{K}$$

### **Resistivity of one dimensional conduction within the water block**

$$\rho_k = \frac{1}{k} = \frac{1}{167} = 0.005988 \text{ mK/W}$$

### **Resistivity of convective heat transfer on GPU die**

$$\rho_h = \frac{1}{h} = \frac{1}{284} = 0.00351 \text{ m}^2\text{K/W}$$

The thermal network of this system is outlined as follows. The conduction through the thermal interface material and aluminium water block from each GPU component is modelled in parallel. Similarly, the water block temperature ( $T_{WB}$ ) to the coolant temperature ( $T_c$ ) are the four convective heat transfer components associated with the convective dissipation over the components. From the coolant perspective, these resistances will be encountered sequentially and will dissipate heat in series; however, from a system perspective, they will be modelled as contributing in parallel between the block and coolant.

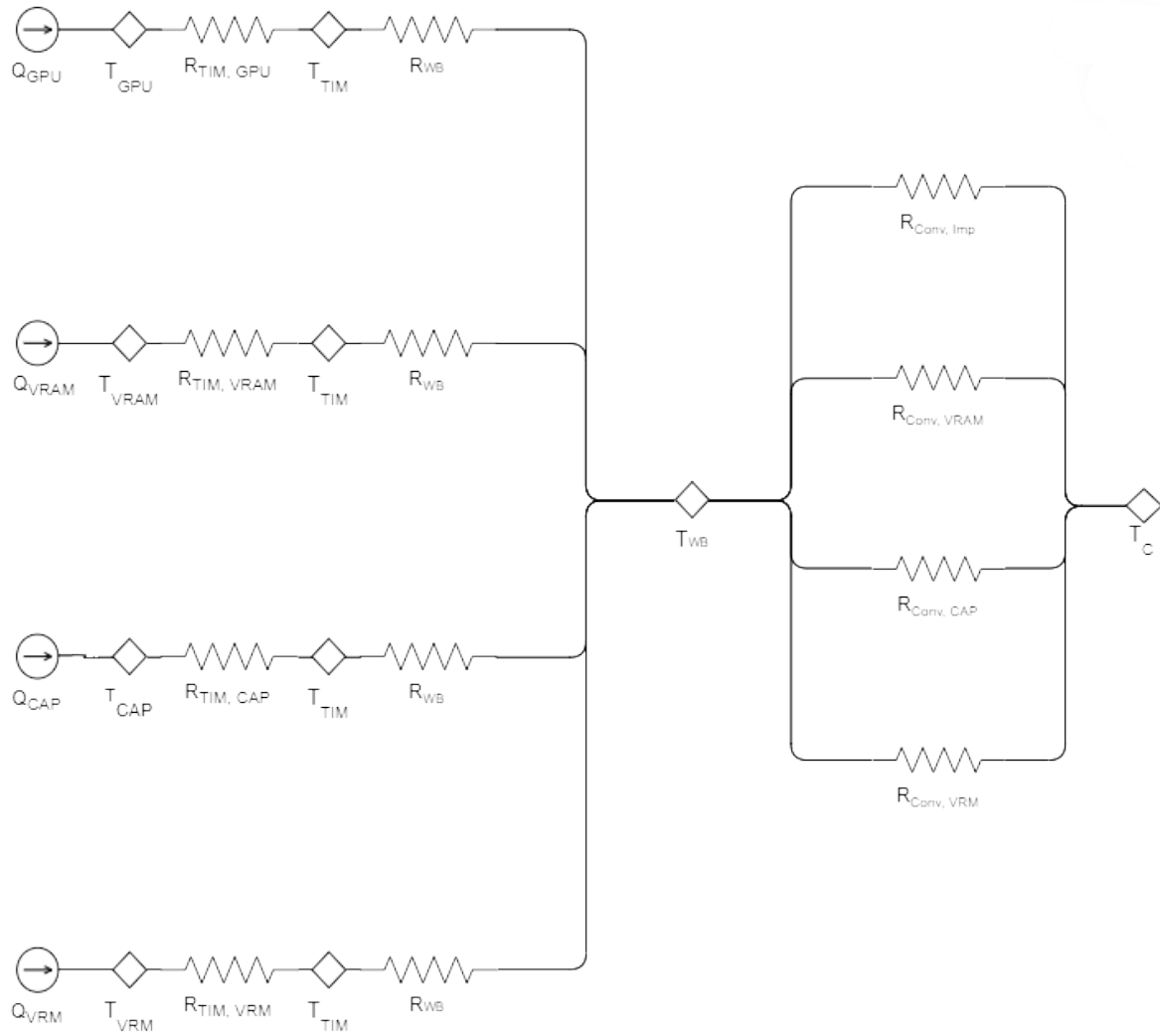


Figure A1.1: Thermal Network Diagram

## Thermal Resistance Calculations

To analytically sense check the CFD results for the GPU die thermal performance, the GPU to coolant thermal pathway was calculated to derive the chip temperature which could then be sense checked against the cad. To do this, the pathway containing the GPU TIM, base plate, and impinging jets thermal resistances were isolated in series. In reality the contributions of the other convective resistances and ambient dissipation will be sources of error in this analysis.

### Given Values

- Thermal Conductivities:

- $k_{TIM} = 17 \text{ W/mK}$

- $k_{\text{TIM, GPU}} = 160 \text{ W/mK}$
- $k_{\text{WB}} = 155.5 \text{ W/mK}$

- **Thicknesses:**

- $L_{\text{TIM, VRM \& CAP}} = 0.5 \text{ mm} = 0.0005 \text{ m}$
- $L_{\text{TIM, VRAM}} = 2.05 \text{ mm} = 0.00205 \text{ m}$
- $L_{\text{TIM, GPU}} = 1 \text{ mm} = 0.001 \text{ m}$
- $L_{\text{WB}} = 1 \text{ mm} = 0.001 \text{ m}$

- **Areas:**

- $A_{\text{GPU}} = 648 \text{ mm}^2 = 6.48 \times 10^{-4} \text{ m}^2$
- $A_{\text{VRAM}} = 1937.3 \text{ mm}^2 = 1.9373 \times 10^{-3} \text{ m}^2$
- $A_{\text{CAP}} = 1981.66 \text{ mm}^2 = 1.98166 \times 10^{-3} \text{ m}^2$
- $A_{\text{VRM}} = 1484.08 \text{ mm}^2 = 1.4841 \times 10^{-3} \text{ m}^2$

## Overall Thermal Network

**Total Chip Resistance (Parallel Network):**

$$\frac{1}{R_{\text{chip}}} = \frac{1}{R_{\text{GPU}}} + \frac{1}{R_{\text{VRAM}}} + \frac{1}{R_{\text{CAP}}} + \frac{1}{R_{\text{VRM}}}$$

**Total Coolant Resistance (Parallel Network):**

$$\frac{1}{R_{\text{coolant}}} = \frac{1}{R_{\text{conv, GPU}}} + \frac{1}{R_{\text{conv, VRAM}}} + \frac{1}{R_{\text{conv, CAP}}} + \frac{1}{R_{\text{conv, VRM}}}$$

## Isolated GPU Network Thermal Resistances

**GPU TIM Resistance:**

$$R_{\text{TIM, GPU}} = \frac{L_{\text{TIM, GPU}}}{k_{\text{TIM, GPU}} \cdot A_{\text{GPU}}} = \frac{0.001}{160 \cdot (6.48 \times 10^{-4})} = 0.00965 \text{ K/W}$$

**GPU Water Block Resistance:**

$$R_{\text{WB, GPU}} = \frac{L_{\text{WB}}}{k_{\text{WB}} \cdot A_{\text{GPU}}} = \frac{0.001}{155.5 \cdot (6.48 \times 10^{-4})} = 0.00992 \text{ K/W}$$

## GPU Convective Resistance

$$R_{\text{conv, GPU}} = \frac{1}{h_{\text{GPU}} \cdot A_{\text{GPU}}} = \frac{1}{33,613 \cdot (6.48 \times 10^{-4})} = 0.0459 \text{ K/W}$$

## Total Component Resistances

GPU Resistance:

$$R_{\text{GPU}} = R_{\text{TIM, GPU}} + R_{\text{WB, GPU}} + R_{\text{conv, GPU}} = 0.00965 + 0.00992 + 0.0459 = 0.06547 \text{ K/W}$$

## GPU Temperature Calculation

Given:

- Coolant temperature:  $T_{\text{coolant}} = 27^\circ C$
- GPU power dissipation:  $Q_{\text{GPU}} = 130 \text{ W}$
- GPU thermal resistance:  $R_{\text{GPU}} = 0.06547 \text{ K/W}$

Using the thermal resistance equation:

$$T_{\text{GPU}} = T_{\text{coolant}} + Q_{\text{GPU}} \cdot R_{\text{GPU}}$$

Substituting the values:

$$T_{\text{GPU}} = 27 + (130 \cdot 0.06547) = 27 + 8.51 = 35.51^\circ C$$

## A2 Appendix B

### A2.1 Preliminary Design Considerations

#### A2.1.1 Jet Design

The effect of the number of jets on the heat transfer coefficient for the jets was estimated by referring to Robinson J. [3]. The heat transfer coefficient ( $h$ ) was estimated using the Nusselt number ( $Nu$ ), thermal conductivity ( $k$ ), and diameter of jets as follows,

$$h = \frac{Nu \cdot k}{d} \quad (\text{A2.1})$$

Nusselt Number was estimated using the following equation,

$$Nu = 1.485 Re_d^{0.46} \left( \frac{S}{d} \right)^{-0.442} Pr^{0.4} \quad (\text{A2.2})$$

Where  $Pr$  is the Prandtl number, whereas the Reynolds number was estimated using jet velocity ( $V_d$ ) and kinematic viscosity ( $\nu$ ) as follows,

$$Re_d = \frac{V_d}{\nu} \quad (\text{A2.3})$$

and

$$V_d = \frac{4\dot{V}}{N\pi d^2} \quad (\text{A2.4})$$

When tested with the diameter of 1, 2, and 3 mm jets, it was observed that the smaller the diameter of the jets, the higher the pressure drop observed, and the lower was the heat transfer. Fig. A2.1 shows the exact relation and matches with the prediction of Robinson J. [3].

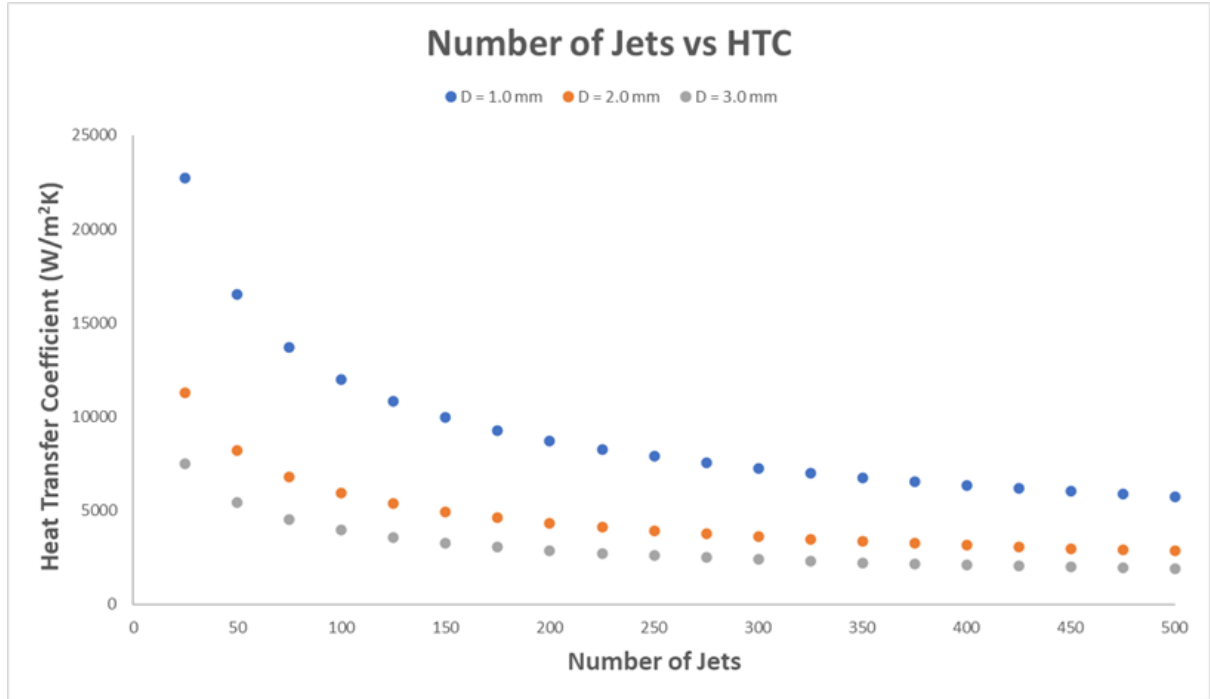


Figure A2.1: Number of Jets vs Heat Transfer Coefficient

As mentioned in section 2.3.1, we decided to move ahead with a 1.5 mm jet diameter, with dimples to enhance heat transfer between the block and coolant. Though dimples were not considered during analytical estimations, we expected a higher heat transfer coefficient. Detailed comparison can be seen in fig.A2.2. This was briefly discussed in 2.3.4, that for the ideal point, estimated coefficient was around 33831.75 W/m<sup>2</sup>K, whereas the CFD result shows it to be 38413.114 W/m<sup>2</sup>K. This gap is supposed to be due to the presence of dimples which were added to increase surface area and promote vortex formation. As it increases surface area, it improves the heat transfer coefficient as well. The max error was observed to be 9300 W/m<sup>2</sup>K for a mass flow of 0.0348 kg/s whereas for the ideal point, the error was 5041.602 W/m<sup>2</sup>K. This indicates that having dimples significantly improves the heat transfer coefficient even at high flow rates. Further optimizing these dimples can improve the heat transfer rate even further, improving the thermal efficiency of the block.

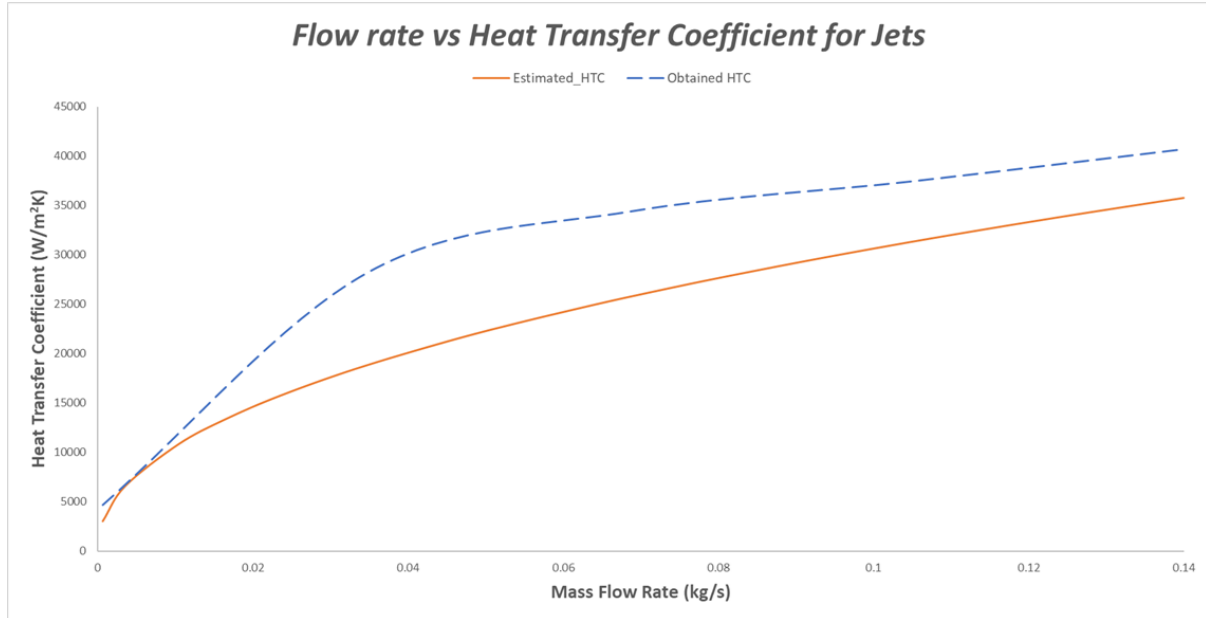


Figure A2.2: Estimated and Obtained Heat Transfer Coefficient for Jets

## A2.2 Fluid Selection

These results were obtained by assuming the working fluid was water, which is inexpensive and works really well. We also tried a water-glycol mixture with varying mixture percentages of glycol from 30% to 50% and observed that the pressure drop was lower compared with only water and had a high heat carrying capacity, but as we were using aluminium as a cooling block, we dropped the idea as it was corrosive without any additives for aluminium and copper. And the design is for gamers and overclockers; it will not use the full potential of the water-glycol mixture, which is a very large temperature band.

Other GPU coolant brands were also considered, which will increase upfront costs for consumers, so they were not tested but still are a viable option.

## A2.3 Previous Geometry and Pressure Drop Estimation

We took a simple approach to make sure the simulations work and carve out a simple path for fluid, which was further modified to obtain the current CAD model. It was a simple model without any jets to plot out the flow. Following fig.A2.3 is the simplified/initial geometry used.

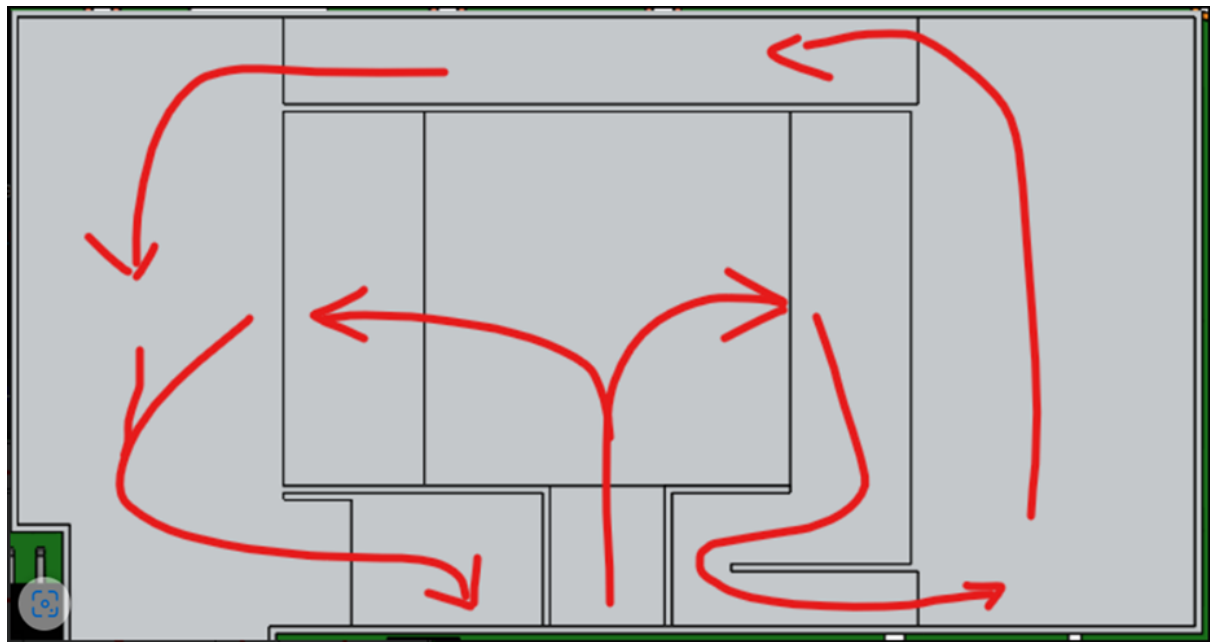


Figure A2.3: Simple geometry with flow paths

Finalized GPU block was modified taking the old geometry into consideration and modified to have a lot more channels diverging and merging together, which allows us to produce turbulence with minimum pressure loss and allows liquid to cover more surface area, but it also made it a bit challenging to estimate the pressure drop across the block. So the fluid path was broken down into sections as seen in fig.A2.4.

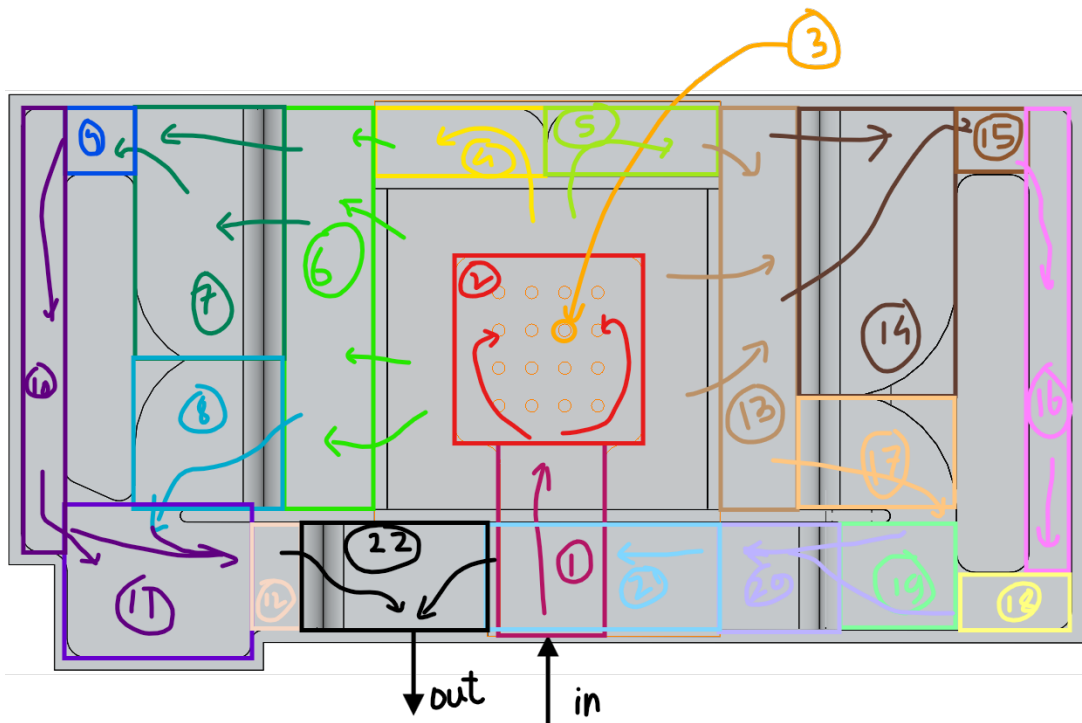


Figure A2.4: Final geometry with sections assumed to calculate pressure drop

Once the sections were formed, their length, width, and height were taken into consideration to calculate the hydraulic diameter. Once dimensions were taken into consideration, pressure drop was calculated using eq.2.4 and eq.2.5. The Minor Loss coefficient was assumed to be 0.05 for gradual contraction and 0.1 for gradual expansion, as the sections 6, 12, 13, and 19 outlets have sections that are curved, leading to this assumption. The results can be seen for old and finalized geometry at fig.A2.5 and can be compared with CFD results in fig.2.14.

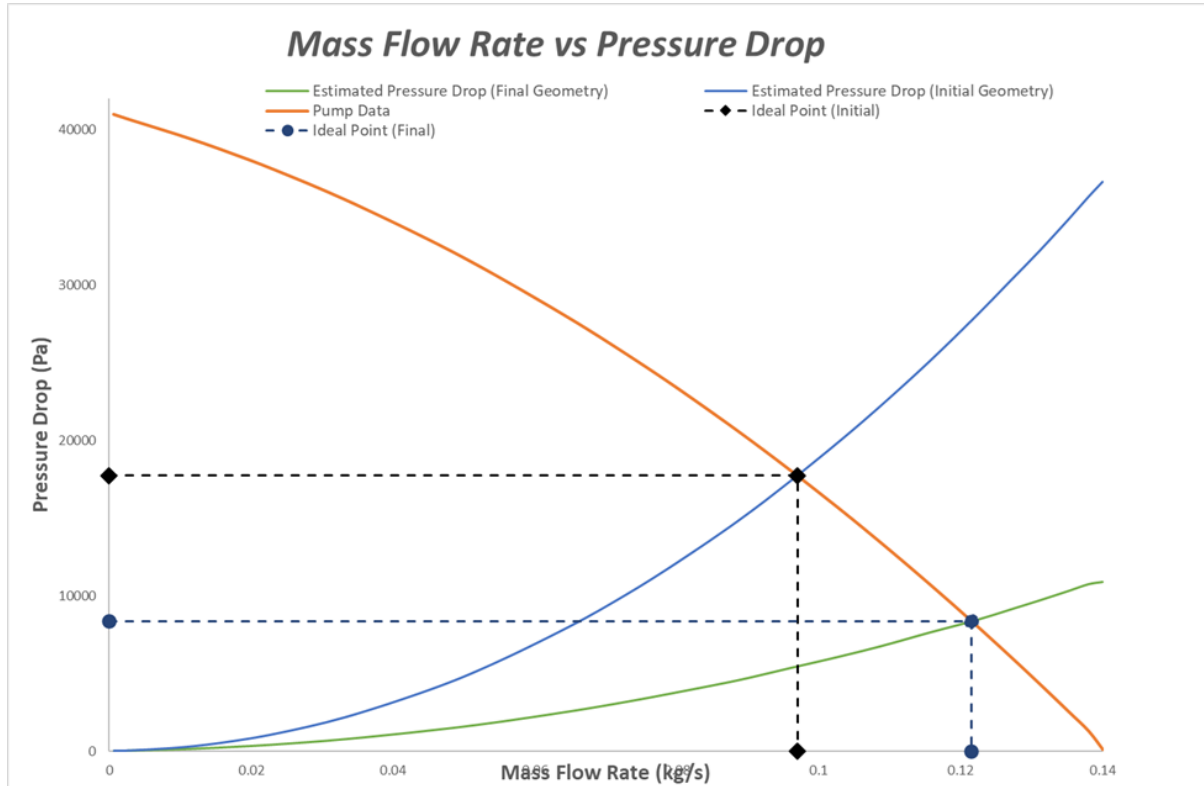


Figure A2.5: Estimated Pressure drop for both initial and final geometries (Working Fluid = Water)

## A3 Appendix C

### A3.1 CFD Results

Mass Flow (kg/s)	Global Temp (°C)	GPU Temp (°C)	HTC (W/m <sup>2</sup> K)	P <sub>in</sub> (Pa)	P <sub>out</sub> (Pa)	dP (Pa)
0.00065	79.14	75.4	4652.995	101325.81	101325	0.81
0.0348	42.7	41.31	28201.567	102088.79	101325	763.79
0.069	39.58	38.37	34425.573	104246.43	101325	2921.43
0.105	38.43	37.33	37440.686	108525.3	101325	7200.3
0.14	36.79	35.85	40694.329	113169	101325	11844

Table A3.1: CFD Results

As shown in table A3.1 results illustrate a clear trend where an increase in mass flow rate leads to a decrease in both Global and GPU temperatures, suggesting that higher flow rates enhance the cooling efficiency of the system. The Heat Transfer Coefficient (HTC) also shows an upward trend with increasing mass flow, which is indicative of more effective heat transfer from the GPU to the coolant. However, while the pressure remains relatively stable, the differential pressure ( $\Delta P$ ) varies significantly with flow rates, indicating that the flow rate adjustment can influence the system's operational pressures.

Mass Flow (kg/s)	Global Temp (°C)	GPU Temp (°C)	HTC (W/m <sup>2</sup> K)	P <sub>in</sub> (Pa)	P <sub>out</sub> (Pa)	dP (Pa)
0.12	37.31	36.3	38413.114	110355.88	101325	9030.88

Table A3.2: Ideal Point

The ideal point highlighted in As shown in table A3.2, with a mass flow of 0.12 kg/s, achieves notably lower temperatures, which might represent the most balanced configuration between cooling performance and pressure management.

## A3.2 Future Optimization Work

While the results from our computational fluid dynamics (CFD) simulations for the cooling system are promising, there are opportunities to further enhance performance by optimizing geometric parameters for orifice geometry. The specific ratios and configurations of these parameters are detailed extensively in Table A3.3 and in Figure A3.2.

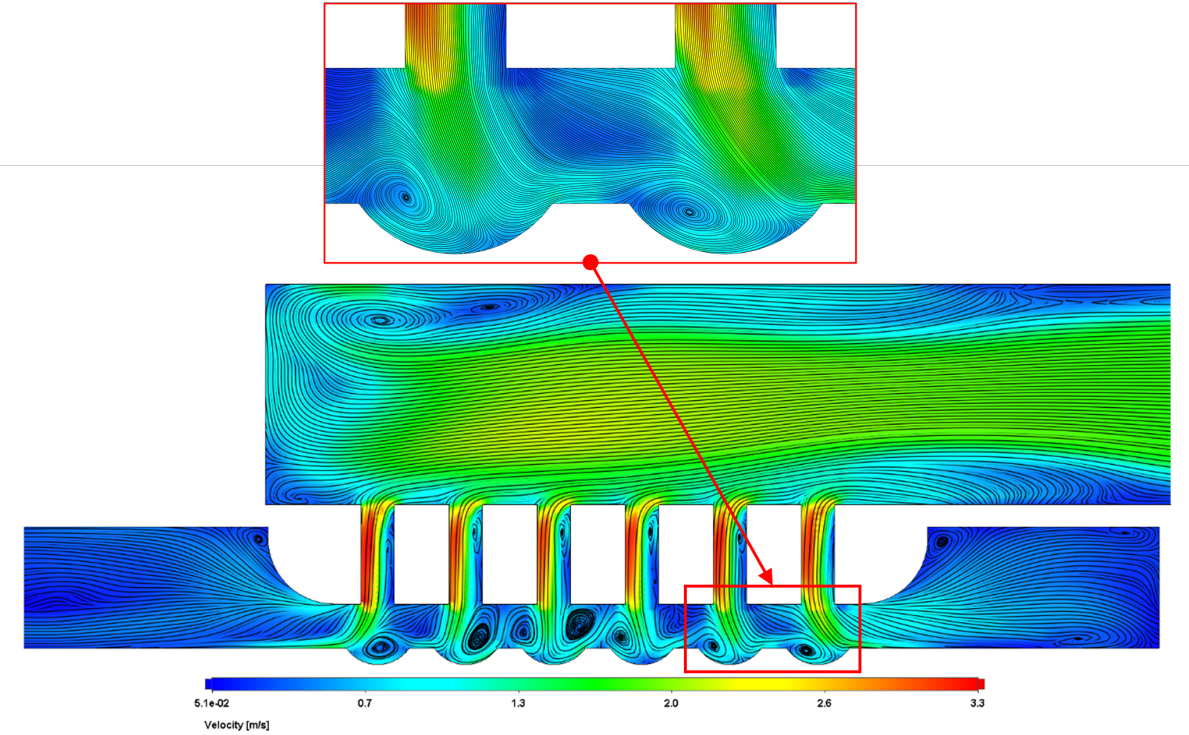


Figure A3.1: Sectioned plot of Velocity

The attached velocity plot illustrates the formation of vortices in the regions at the dimples of the cooling channels, which indicates that the flow is being diverted significantly. This diversion can reduce the effectiveness of heat transfer from the GPU surface. By reducing the height-to-diameter ratio ( $H/D$ ) as shown in the Figure A3.2, we can improve the impact of the cooling jets directly on the heat source. This adjustment aims to minimize the development of vortices and enhance the direct impingement of the cooling flow onto critical areas, thus optimizing the removal of heat.

Parameter	Description	Unit	Value
D	Jet diameter	mm	1.50
S/D	Jet spacing ratio	-	2
H/D	Jet-target ratio	-	1.33
N	Jet population	-	36

Table A3.3: Geometric Variables

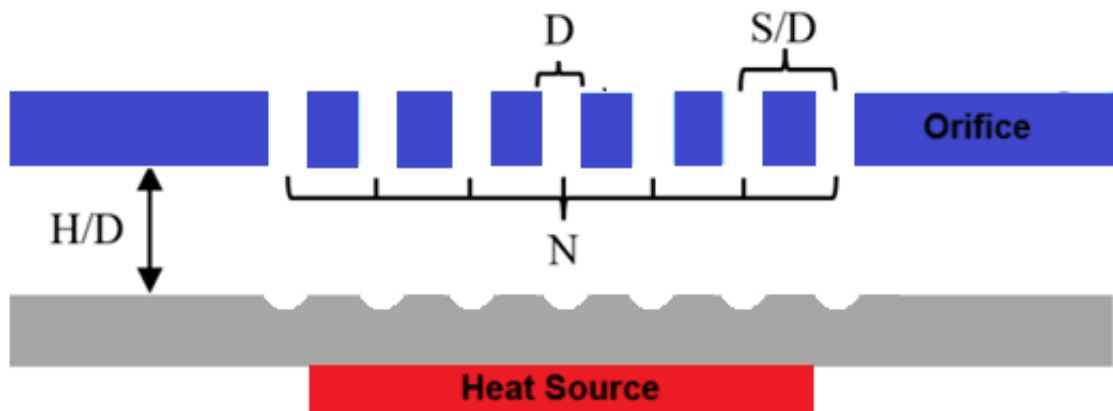


Figure A3.2: Sectioned orifice plate, highlighting geometric variables

Further optimization work can be undertaken to refine this aspect of the design. By tweaking the spacing and diameter of the nozzles (S/D and D parameters), along with the jet's impact height, we can fine-tune the flow dynamics to maximize cooling efficiency while minimizing flow resistance. This will ensure that the cooling system not only maintains low GPU temperatures but also operates with enhanced energy efficiency, aligning with both performance requirements and aesthetic values desired in high-end gaming systems.

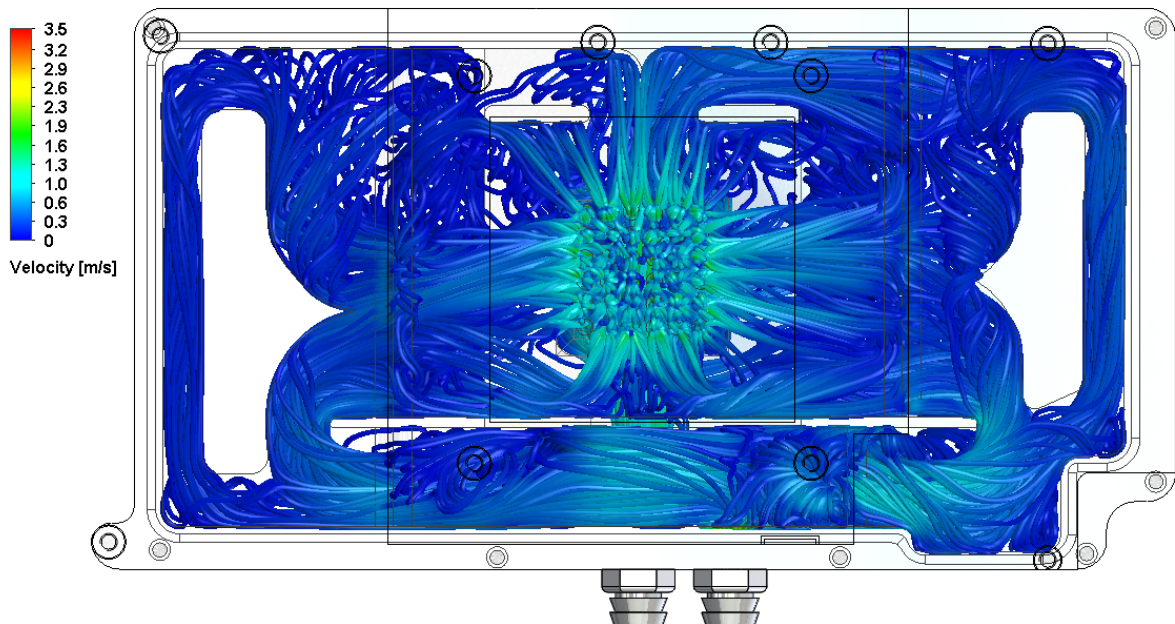


Figure A3.3: Bottom view of water block for Velocity